

Nicole J. Crane,^{1,*} Ph.D.; Edward G. Bartick,² Ph.D.; Rebecca Schwartz Perlman,² Ph.D.; and Scott Huffman,^{3,†} Ph.D.

Infrared Spectroscopic Imaging for Noninvasive Detection of Latent Fingerprints

ABSTRACT: The capability of Fourier transform infrared (FTIR) spectroscopic imaging to provide detailed images of unprocessed latent fingerprints while also preserving important trace evidence is demonstrated. Unprocessed fingerprints were developed on various porous and nonporous substrates. Data-processing methods used to extract the latent fingerprint ridge pattern from the background material included basic infrared spectroscopic band intensities, addition and subtraction of band intensity measurements, principal components analysis (PCA) and calculation of second derivative band intensities, as well as combinations of these various techniques. Additionally, trace evidence within the fingerprints was recovered and identified.

KEYWORDS: forensic science, latent fingerprints, FTIR, spectroscopic imaging, trace evidence

While many techniques are established for a particular forensic evaluation, specific analyses require re-examination and further research for two primary reasons. First, there is the need to develop techniques to reduce the time expended in performing an analysis, and, second, improvements in analytical methodologies are required for providing more reliable, unambiguous results. Developing new analytical approaches and conducting validation studies assure that the most reliable forensic evidence will be entered into the justice system.

In 1999, the U.S. Department of Justice published a document entitled "Forensic Sciences: Review of Status and Needs" (1). One of the sections in this publication was dedicated to "Methods Research, Development, Testing and Evaluation." The current status and needs were listed for nine areas of forensic science, including latent fingerprint examinations. According to the document, latent fingerprints require "improved recovery and visualization methods and detection of associative evidence in prints."

Latent fingerprints present a considerable challenge in forensics, as invasive methods are often required for developing a print. Processing techniques for fingerprints include chemicals, powders, and/or various light sources (2–6), which may damage or destroy chemical associative trace evidence within the fingerprint. Thus, a noninvasive procedure that captures a digital image of the fingerprint, along with the chemical information within that fingerprint, adds significantly to the tools available to the forensic scientist.

Recently, the application of visible absorption and luminescence spectroscopic imaging studies on latent fingerprint detection has produced promising results (7–10). With visible imaging, the detection of untreated latent prints on substrates such as acetate sheets and a white plastic bag was possible (9). The authors indicated that ridge detail was detected on untreated yellow paper. However, sufficient detail was not observable to discern the ridge characteristics for identification. Visible imaging proved more successful on treated substrates such as newspaper, money, glass, a drug bag, and a plastic Ziplock[®] (S.C. Johnson Racine, WI) bag. In these instances, the detection is not exclusively of the fingerprint but rather the chemicals used to treat the latent prints. Associative trace evidence contained within the print may be compromised because of the chemical treatment. In addition, the detection of the latent prints is based on broad visible absorptions that are not chemical component specific.

Unlike visible spectroscopy, mid-infrared (IR) spectroscopy is based on molecular absorptions that are characteristic of specific molecular structure resulting from the chemical composition of the material being studied. Bartick et al. (11) and Williams et al. (12) used single detector Fourier transform infrared (FTIR) microspectroscopy to characterize the chemical composition of the various residues contained in adult and child fingerprints. The chemistry of these residues varies among individuals and contains both eccrine deposits from the fingers alone and sebaceous deposits resulting from the depositor having previously touched various body parts, such as the face or neck. Both classes of deposits consist of fatty acid esters, protein from skin particles, and carboxylic acid salts, while sebaceous material consists primarily of esters. As a person reaches puberty, fingerprints often contain a higher concentration of sebaceous matter. A representative IR spectrum, shown in Fig. 1 with associated band assignments listed in Table 1 (13), illustrates the ability to discern critical chemical components.

Single detector IR spectroscopy is a common technique for the identification of materials. IR is very useful in forensic applications, such as for trace evidence and for drug analysis, by discerning both the organic and inorganic components of the samples (14,15). IR spectroscopy may be implemented in an imaging

¹Oak Ridge Institute for Science Education, FBI Laboratory, Counterterrorism and Forensic Science Research Unit, FBI Academy, Quantico, VA 22135.

²FBI Laboratory, Counterterrorism and Forensic Science Research Unit, FBI Academy, Quantico, VA 22135.

³Laboratory of Chemical Physics, NIDDK, National Institutes of Health, Bethesda, MD 20892-0520.

*Present address: Laboratory of Chemical Physics, NIDDK, National Institutes of Health, Bethesda, MD 20892-0520.

†Present address: Department of Chemistry and Physics, Western Carolina University, Cullowhee, NC 28723.

Received 25 Mar. 2006; and in revised form 4 Aug. 2006; accepted 1 Sept. 2006; published 10 Dec. 2006.

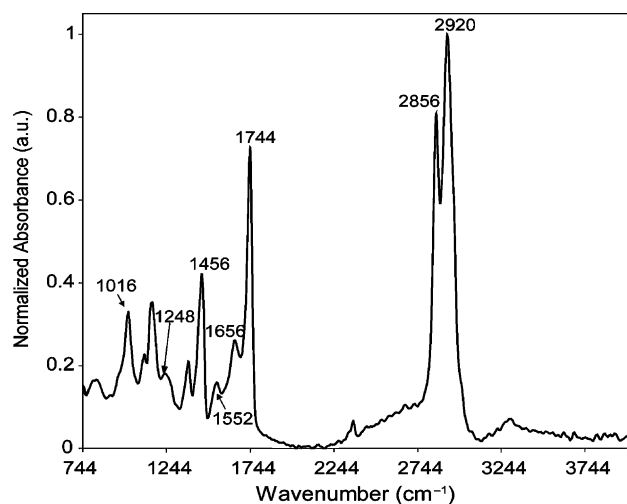


FIG. 1—Infrared spectrum of fingerprint residue on an aluminum slide.

mode for a wide range of applications that include, for example, pharmaceutical tablet examinations and histopathological tissue diagnostics (16–30). IR imaging not only provides a spatial distribution of the component materials, but an identification of individual constituents.

The application of FTIR for imaging of latent fingerprints was first demonstrated by Bartick et al. (11) using spectral bands indicative of the chemical components of the deposited material. The images were from prints deposited on aluminum-coated glass microscope slides for representing a reflective substrate. The detection of an explosive material, RDX, was viewed and spectrally identified in a latent fingerprint composite spectral image deposited on an aluminum-coated slide (31). More recently, in a study by Tahtouh et al., (32) FTIR imaging performed well for the detection of ethyl cyanoacrylate fumed latent prints on polymer banknotes, as well as treated and untreated latent prints on glass. All detection and contrast of the treated latent prints were based on the carbonyl stretching mode of the ethyl cyanoacrylate at 1743 cm^{-1} . The contrast provided by FTIR imaging is clearly superior to that of visible imaging. Our present study demonstrates the ability of IR spectroscopic imaging to reveal latent print details on challenging substrates without preprocessing or pretreating the latent prints. However, in some cases, the print was slightly visible by eye. In either case, processing with IR spectral imaging techniques rendered all prints clearly visible.

TABLE 1—Infrared band assignments for spectrum (Fig. 1) of fingerprint residue (13).

Wavenumber (cm^{-1})	Assignment
1016	Asymmetric O–C–C stretch, ester
1248	Asymmetric C–C–O stretch, ester (C bonded to the O included in the carbonyl)
1456	CH ₂ scissors
1552	N–H bend combined with C–N stretch, protein amide II feature
1656	C = O stretch, protein amide I feature
1744	C = O stretch, saturated ester
2856	Methylene C–H stretch
2920	Methyl C–H stretch

Materials and Methods

FTIR Imaging

Fingerprints were deposited onto substrates after rubbing one's forehead. All substrates were mounted onto MirrIR slides (Kevley Technologies, Chesterland, OH) using clear cellophane tape on the edges of the substrates to secure them to the slides. Substrates included nonporous (trash bags, a soda can, tape) and porous (copier paper, cigarette butt paper, U.S. dollar bill, postcard) materials. An image of the fingerprints on the various substrates was first acquired with a PowerLook III scanner (Techville Inc., Dallas, TX), 1200×2400 dpi (Umax, <http://www.umax.com>). It is important to note that the location of the fingerprints was known before collecting IR images.

Both visible and IR reflectance images were collected using a Spectrum Spotlight 300 FTIR Microscope System, with a $100\text{ }\mu\text{m} \times 100\text{ }\mu\text{m}$ microscope aperture (Perkin Elmer, Shelton, CT). All visible reflectance images of the samples were acquired before the IR image. IR backgrounds for the images were collected in regions of the substrate without fingerprint residue and used the same $4000\text{--}700\text{ cm}^{-1}$ range as the corresponding IR images. The background scan parameters included 120 scans/pixel at 16 cm^{-1} spectral resolution. The regions for the IR images were selected from within the visible reflectance image, as indicated by black and white boxes superimposed on the figures that follow, with sizes varying from $6.48\text{ mm} \times 7.15\text{ mm}$ ($W \times H$) to $23.7\text{ mm} \times 12.8\text{ mm}$. All IR images were collected using the reflectance and image mode with a pixel size of $25\text{ }\mu\text{m}$. IR image parameters included 4 scans/pixel at 16 cm^{-1} spectral resolution. Fingerprint samples were stored for up to 3 months; no spectral degradation of the fingerprints was observed with varying lengths of storage time.

Image Analysis

Once acquired, all spotlight IR images were imported into ENVI[®] software (RSI Inc., Boulder, CO) using an “in-house written” program (available upon request) that converted the Perkin Elmer data format into a data format transferable to ENVI[®]. IR images were analyzed with varying techniques, including band intensity images, addition and subtraction of band intensity images, principal components analysis (PCA, specifically forward PC rotation with new statistics), and second derivative band intensity images, as well as appropriate combinations of these techniques. Both PCA and second derivative calculations for IR image analysis have been discussed in detail elsewhere (33). All data analysis performed in ENVI[®] used programs provided within the software, except the program for calculating second derivative images.

For the band intensity images and second derivative band intensity images, ester bands were commonly used to obtain images of the fingerprint residue. Most images were obtained using the 1016 cm^{-1} asymmetric O–C–C stretch ester vibrational mode. Although the most intense 1744 cm^{-1} carbonyl stretching mode of the ester may also have been used, the weaker 1016 cm^{-1} mode provided images with superior clarity. The reason for the enhanced results using the 1016 cm^{-1} band is not clear to the authors and is under investigation. For data not shown here, comparable images were obtained using additional vibration bands (1552 , 1664 , and 1744 cm^{-1}).

In addition, a reflectance spectrum of a blue, cylindrical fiber on the postcard was acquired. The fiber was removed from the postcard and mounted onto a MirrIR slide via an adhesive fiber holder.

The spectrum was collected over the range of $4000\text{--}700\text{ cm}^{-1}$ at 1 cm^{-1} intervals and a total of 32 scans. The fiber spectrum was automatically baselined and matched to its fiber components in the Perkin Elmer spectrum[®] software (Wellesley, MA) using the FBI fiber library (Version 4.0).

Results and Discussion

The thickness of the substrates required that images be determined in reflectance mode. For this experiment, the soda can sample was deemed to be the simplest substrate because its aluminum sheet with paint would promote the greatest reflectance. An untreated fingerprint deposited onto a Dr. Pepper's[®] (Cadbury Schweppes Americas Beverages, Plano, TX) soda can is shown in Fig. 2A. While the fingerprint on the soda can is visible with the visible scanning technique, areas of paint on the can conceal portions of the fingerprint. By plotting the vibrational band intensity at 1016 cm^{-1} (Fig. 2B), the fingerprint contrast is greatly enhanced. For this example, the use of additional mathematical algorithms is not necessary, as an image based on band intensity is all that is required.

Figure 3A shows an untreated fingerprint deposited onto a black trash bag. This substrate is more challenging as the substrate is less reflective and is not flat. In spite of these challenges, Fig. 3B displays a virtually unobstructed fingerprint image based on the 1016 cm^{-1} band intensity. Again, complicated algorithms were not required for fingerprint visualization. Areas of the image where wrinkles were present appear smudged on the IR image, but adequate fingerprint detail is retained for these areas.

Duct tape is a more heterogeneous substrate compared with a soda can or trash bag. As duct tape contains a plastic and woven backing, as well as adhesive, and as it is not completely flat, variations are noted in the image profile. The brand of tape shown in Fig. 4A does not have the typical silver color of duct tape but ra-



FIG. 2—Cut and flattened Dr. Pepper's soda can with fingerprint deposit. (A) Soda can imaged by a document scanner. (B) Infrared image of the outlined area obtained by plotting the band intensity at 1016 cm^{-1} .

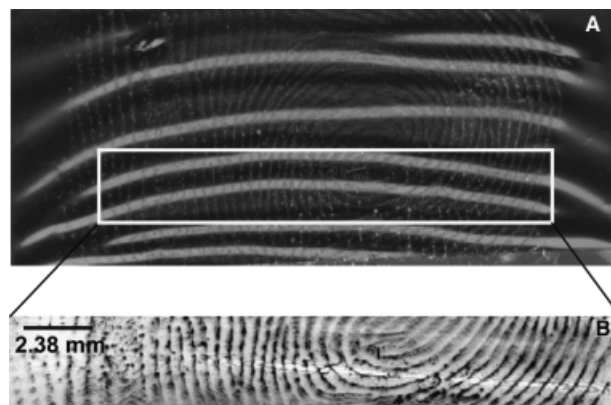


FIG. 3—Black, plastic garbage bag with a fingerprint, taped flat. (A) Trash bag imaged by a document scanner. (B) Infrared image of the outlined area obtained by plotting the band intensity at 1016 cm^{-1} .

ther a nonreflective, semitransparent yellow color. Simple plotting of band intensity for imaging is not successful for this particular substrate; thus, further mathematical processing is required. By subtracting the band intensity image of the tape at 696 cm^{-1} from the band intensity image of the fingerprint residue at 1016 cm^{-1} , a fingerprint is visible on the tape without the use of chemicals, as can be seen in Fig. 4B. Unlike the previous examples presented here, FTIR imaging was able to develop a print spectroscopically that was not otherwise visible.

Paper, due to its porosity, represents a challenging substrate for the spectroscopic development of fingerprints. For example, fingerprint residue is barely visible on the unprocessed white copier paper shown in Fig. 5A. Until now, the examples discussed for obtaining fingerprint images have been from nonporous materials. Porous materials like paper have low reflectivity, are absorbent,

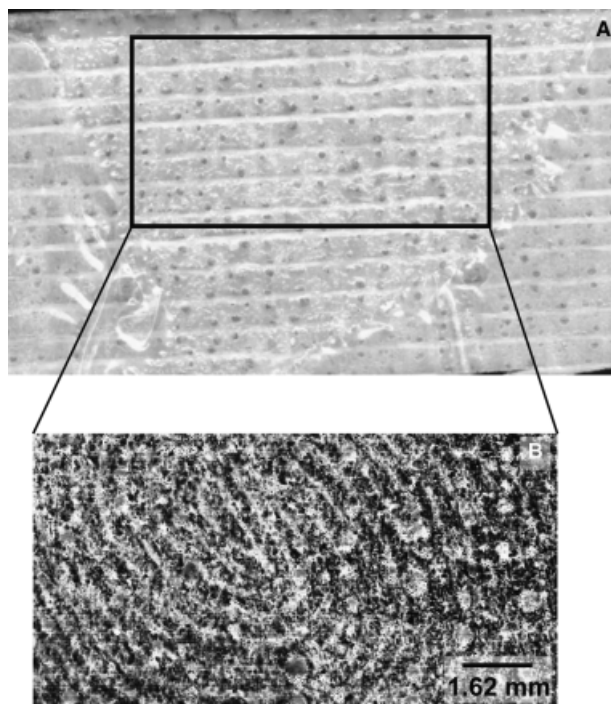


FIG. 4—Fingerprint deposited onto a duct tape-like tape. (A) Tape imaged by a document scanner. (B) Infrared image of the outlined area obtained by band math, the subtraction of the band intensity at 696 cm^{-1} from the band intensity at 1016 cm^{-1} .

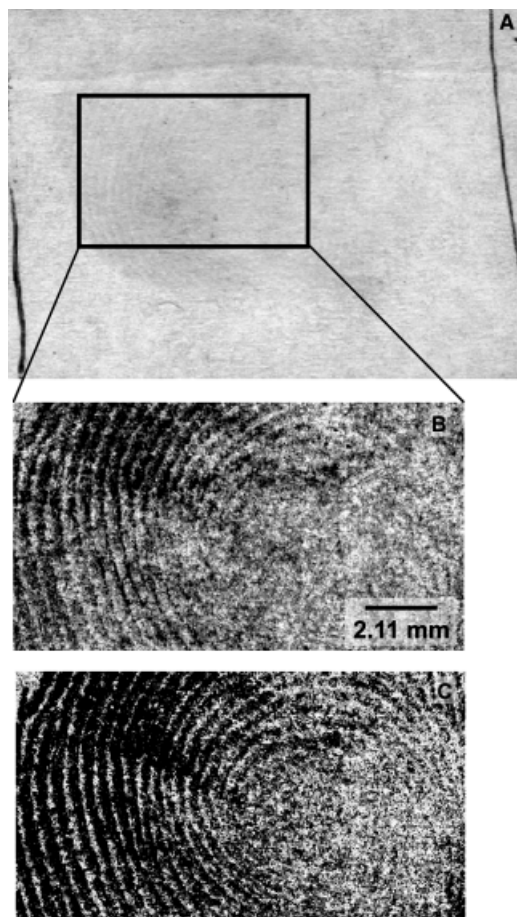


FIG. 5—Fingerprint deposited onto white copier paper. (A) Copier paper with fingerprint as imaged by a document scanner. (B) Infrared image outlined area obtained using principal components analysis. (C) Infrared image outlined area from second derivative spectral band intensity at 1016 cm^{-1} .

and heterogeneous (nonuniform distribution and orientation of paper fibers). The application of band intensity images was not sufficient for rendering this fingerprint visible. For this example, two methods were compared: PCA and second derivatization. PCA calculations are performed to extract component spectra and have been frequently used for spectral imaging enhancement (8,10,34). The PCA-derived image is shown in Fig. 5B. Although a partial fingerprint is revealed, a portion remains obscured by the paper fibers. Figure 5C shows a successful depiction of the entire fingerprint on the copier paper. The fingerprint in Fig. 5C was obtained by performing a second derivative calculation on all of the spectra in the image and then by plotting the band intensity at 1016 cm^{-1} . The second derivative calculations provided superior results compared with PCA for two reasons. First, because PCA calculates the principal components of the image based on spectral variation, the fingerprint becomes less visible in the lower right areas of Fig. 5A and B. Second, by minimizing background features in the spectrum, such as the broad spectral interference from paper, the second derivative of the spectrum allows the narrow spectral features to become prominent.

Cigarette butt paper differs from that of copier paper because it is more porous. Figure 6A shows the cigarette butt paper removed from the filter and flattened onto a microscope slide. Note that the fingerprint is not at all visible. Merely plotting the band intensity at 1016 cm^{-1} was inadequate for fingerprint development; however, once the second derivative spectra were calculated and the

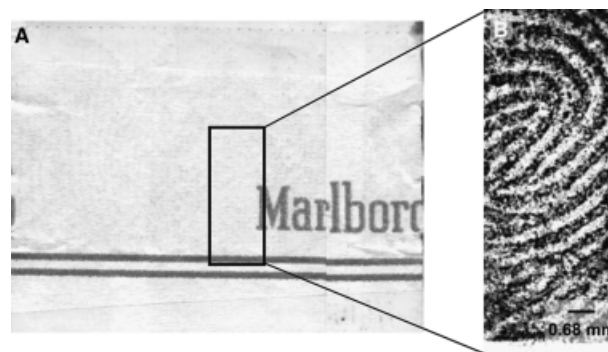


FIG. 6—Cigarette butt paper removed from cigarette filter, flattened, and deposited with fingerprint. (A) Cigarette butt paper as imaged by a document scanner. (B) Infrared image of outlined area by using the second derivative band intensity at 1016 cm^{-1} .

band intensity was again plotted for the 1016 cm^{-1} feature, the fingerprint was clearly observed (Fig. 6B) with no interference from the paper substrate.

Paper money may present difficulties as the substrate contains not only paper, but various inks, foils, and fibers. A scanned image of a portion of a U.S. one dollar bill is shown in Fig. 7A. A fingerprint is not visible on the scanned image of the bill; however, calculation of second derivative spectra and a plot of the 1016 cm^{-1} band intensity reveal a fingerprint (Fig. 7B). Figures 7C and D show components isolated within the bill. On the U.S. dollar bill, the number “3” and the border design are black in color. By simple visual inspection, it is not clear whether the number “3” and the border design are derived from the same ink. However, from the addition and subtraction of various band intensity images, we note that the number “3” and the border design are representative of two different inks. This type of spectral differentiation would be useful to characterize counterfeit money. Thus, evidence is more valuable because there is not only the possibility of counterfeit identification but also a direct link and possible identification of the criminal if a fingerprint is present.

The last example of IR imaging for non-invasive fingerprint detection involves a postcard (Fig. 8A). Upon visual inspection, the fingerprint appears somewhat smeared and little detail is retained. Fortunately, the postcard has the advantage of a semi-glossy coating, which increases the overall reflectance of the substrate. However, the substrate is a semiporous cardboard-like material with four different inks in various layers. The use of PCA enabled us to separate the postcard into its various components, revealing at least three of the inks and, most importantly, the fingerprint (Fig. 8B).

Within the small circle in Fig. 8A appears a blue fiber. This is an instance when the initial evidence contains additional associative evidence. By developing the fingerprint noninvasively, the fiber can be spectroscopically analyzed. By using another print development technique, the chemicals used may have obscured the spectral “fingerprint” of the fiber itself. In this case, the fiber was removed from the postcard and analyzed using single detector FTIR spectroscopy. The fiber was rolled and mounted onto a reflective glass slide. The blue, cylindrical fiber has a diameter of approximately $25\text{ }\mu\text{m}$ (Fig. 9A). Several spectra were collected along various locations on the fiber shaft. After comparing the fiber spectrum with the FBI fiber database, the fiber was identified as likely being rayon (Fig. 9B). Additional peaks in the spectrum that are not evident in the spectrum of rayon likely result from fingerprint residue, thus suggesting that the fiber should have been

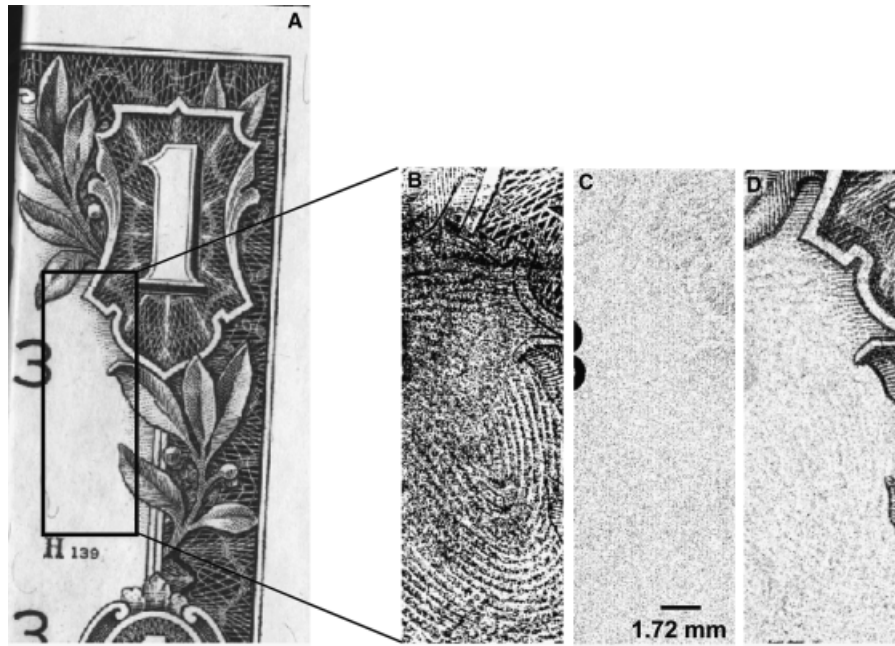


FIG. 7—U.S. dollar bill with a latent print. (A) Scanned image of a U.S. one dollar bill. (B) Infrared image of the outlined area of a dollar bill, revealed by using the second derivative band intensity at 1016 cm^{-1} . Isolation of the number "3" (C) and border design (D) on the bill obtained by second derivative band math.

cleaned. The cylindrical morphology of the fiber supports the identification of the fiber as rayon over cotton with a cellulose component material.

Other substrates examined, but not presented in this manuscript, were glass, double-sided clear cellophane tape, electrical tape, an opaque white tape with orange printing, a white, opaque trash bag, a white, translucent trash bag, a plastic knife handle, green-colored copier paper, a magazine page, cigarette shaft paper, cardboard, a Kimwipe[®] (Kimberly-Clark Corp., Neenah, WI) tissue, and, overlapping prints on a manila envelope. Latent prints were detected on all of the above substrates, except for cardboard and the Kimwipe[®] tissue, perhaps because of the porosity and fibrous

nature of these two materials. Individual overlapping prints on the manila envelope were resolved, using spectral differences in the second derivative spectra of the fingerprint residues.

Conclusion

In this study, FTIR imaging was used for the noninvasive detection of latent fingerprints and was accomplished in such a

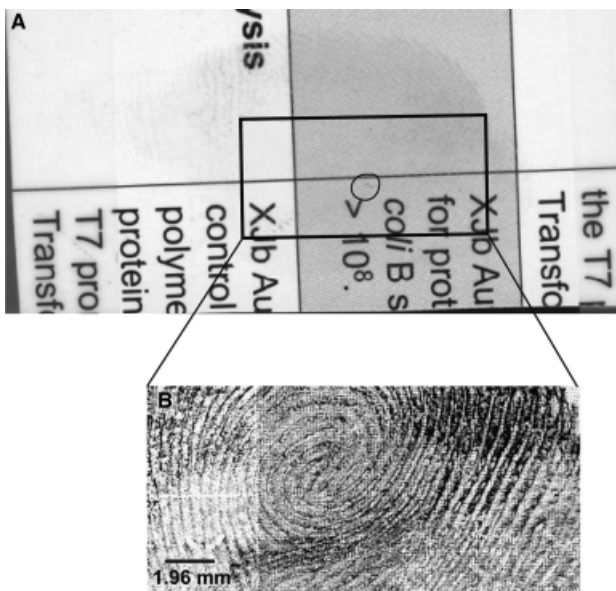


FIG. 8—Postcard with latent print. (A) Scanned image of postcard. Note the fiber (blue in color) on the postcard, denoted by the circle. (B) Infrared image of outlined area, obtained by principal components analysis.

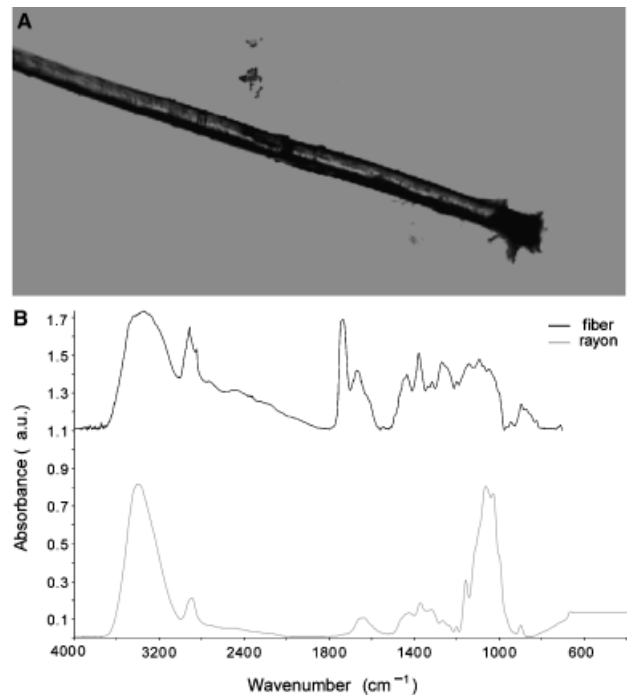


FIG. 9—(A) Image of fiber removed from postcard, as seen by a color charge coupled device camera on an infrared microscope. (B) Spectral comparison of blue fiber with Federal Bureau of Investigation fiber database rayon fiber.

manner as to preserve trace evidence associated with the prints. This enables the analyst to make a direct connection between the fingerprint and the trace evidence without altering the state of the evidence. Untreated latent prints on various nonporous and porous substrates were imaged. Various analysis techniques, including band intensity, addition and subtraction of band intensity, PCA, and second derivative band intensity, were utilized to improve the print images on the substrates. In addition to detecting prints, additional forensic information was obtained using FTIR. For example, a fiber was found and identified within a fingerprint on a postcard. In addition to the latent print detected on paper money, different chemical components characterizing the inks on the bill were also indicated.

In general, this method works well when one knows where to look for latent fingerprints. With work toward validating the methods demonstrated here, case work applications appear viable. Additionally, future studies are being considered for further instrumental development where IR imaging could be used as a field technique for the noninvasive detection of both latent fingerprints and trace evidence.

Acknowledgments

The authors would like to thank Rohit Bhargava for his programming assistance. We would also like to thank Ira W. Levin for his helpful discussions on this particular study. The authors would also like to acknowledge partial support from the Intramural Research Program of the National Institute of Diabetes and Digestive and Kidney Diseases.

References

- U.S. Department of Justice. Forensic sciences: review of status and needs. Gaithersburg, MD: AS Corporation, 1999:1–71.
- Brettell TA, Rudin N, Saferstein R. Forensic science. *Anal Chem* 2003;75(12):2877–90.
- Roorda RD, Ribes AC, Damaskinos S, Dixon AE, Menzel ER. A scanning beam time-resolved imaging system for fingerprint detection. *J Forensic Sci* 2000;45(3):563–7.
- Bouldin KK, Menzel ER, Takatsu M, Murdock RH. Diimide-enhanced fingerprint detection with photoluminescent CdS/dendrimer nanocomposites. *J Forensic Sci* 2000;45(6):1239–42.
- Seah LK, Dinis US, Ong SK, Chao ZX, Murukeshan VM. Time-resolved imaging of latent fingerprints with nanosecond resolution. *Opt Laser Technol* 2004;36(5):371–6.
- Dinis US, Chao ZX, Seah LK, Singh A, Murukeshan VM. Formulation and implementation of a phase-resolved fluorescence technique for latent-fingerprint imaging: theoretical and experimental analysis. *Appl Opt* 2005;44(3):297–304.
- Exline DL, Schuler RL, Treado PJ, Corp C. Improved fingerprint visualization using luminescence and visible reflectance chemical imaging. *Forensic Science Communications* 2003 July, <http://www.fbi.gov/hq/lab/fsc/backissu/july2003/exline.htm>.
- Exline DL, Wallace C, Roux C, Lennard CI, Nelson MP, Treado PJ. Forensic applications of chemical imaging: latent fingerprint detection using visible absorption and luminescence. *J Forensic Sci* 2003;48(5):1047–53.
- Payne G, Reedy B, Lennard C, Comber B, Exline D, Roux C. A further study to investigate the detection and enhancement of latent fingerprints using visible absorption and luminescence chemical imaging. *Forensic Sci Int* 2005;150(1):33–51.
- Miskelly GM, Wagner JH. Using spectral information in forensic imaging. *Forensic Sci Int* 2005;155:112–8.
- Bartick E, Schwartz R, Bhargava R, Schaeberle M, Fernandez D, Levin I. Spectrochemical analysis and hyperspectral imaging of latent fingerprints. In: Baccino E, editor. Proceedings of the 16th Meeting of the International Association of Forensic Sciences; 2002 September 2–7; Montpellier, France. Bologna, Italy: Monduzzi Editore, IPD, 2002:61–4.
- Williams D, Schwartz R, Bartick E. Analysis of latent fingerprint deposits by infrared microspectroscopy. *Appl Spectrosc* 2004;58(3):313–6.
- Smith B. Infrared spectral interpretation: a systematic approach. Boca Raton, FL: CRC Press LLC, 1999.
- Suzucki EM. Forensic applications of infrared spectroscopy. In: Saferstein RE, editor. Forensic science handbook. 1st ed. Englewood Cliffs: Prentice-Hall Career and Technology, 1993:71–195.
- Bartick E, Tungol MW. Infrared microscopy and its forensic applications. In: Saferstein RE, editor. Forensic science handbook. 1st ed. Englewood Cliffs: Prentice-Hall Career and Technology, 1993:196–252.
- Fernandez DC, Bhargava R, Hewitt SM, Levin IW. Infrared spectroscopic imaging for histopathologic recognition. *Nat Biotechnol* 2005;23(4):469–74.
- Yu P. Molecular chemistry imaging to reveal structural features of various plant feed tissues. *J Struct Bio* 2005;150(1):81–9.
- Chan KLA, Kazarian SG. Fourier transform infrared imaging for high-throughput analysis of pharmaceutical formulations. *J Combinat Chem* 2005;7(2):185–9.
- Faibish D, Gomes A, Boivin G, Binderman I, Boskey A. Infrared imaging of calcified tissue in bone biopsies from adults with osteomalacia. *Bone* 2005;36(1):6–12.
- Bhargava R, Levin IW. Enhanced time-resolved Fourier transform infrared spectroscopic imaging for reversible dynamics. *J Phys Chem A* 2004;108(18):3896–901.
- Oh SJ, Do JS, Ok JH. Studies of poly(styrene-co-allyl alcohol)/polyester blends using Fourier transform infrared spectroscopy and imaging. *Appl Spectrosc* 2003;57(9):1058–62.
- Boskey AL, Moore DJ, Amling M, Canalis E, Delany AM. Infrared analysis of the mineral and matrix in bones of osteonectin-null mice and their wildtype controls. *J Bone Miner Res* 2003;18(6):1005–11.
- Rafferty DW, Koenig JL. FTIR imaging for the characterization of controlled-release drug delivery applications. *J Control Rel* 2002;83(1):29–39.
- Potter K, Kidder LH, Levin IW, Lewis EN, Spencer RGS. Imaging of collagen and proteoglycan in cartilage sections using Fourier transform infrared spectral imaging. *Arthritis Rheum* 2001;44(4):846–55.
- Harif R, Matz G. Toxic cloud imaging by infrared spectrometry: a scanning FTIR system for identification and visualization. *Field Anal Chem Technol* 2001;5(1-2):75–90.
- Mendelsohn R, Paschalis EP, Sherman PJ, Boskey AL. IR microscopic imaging of pathological states and fracture healing of bone. *Appl Spectrosc* 2000;54(8):1183–91.
- Kidder LH, Colarusso P, Stewart SA, Levin IW, Appel NM, Lester DS, et al. Infrared spectroscopic imaging of the biochemical modifications induced in the cerebellum of the Niemann–Pick type C mouse. *J Biomed Opt* 1999;4(1):7–13.
- Schultz CP, Liu KZ, Kerr PD, Mantsch HM. In situ infrared histopathology of keratinization in human oral/oropharyngeal squamous cell carcinoma. *Oncol Res* 1998;10(5):277–86.
- Paschalis EP, Recker R, DiCarlo E, Doty S, Atti E, Boskey AL. Distribution of collagen cross-links in normal human trabecular bone. *J Bone Miner Res* 2003;18(11):1942–6.
- Garidel P. Mid-FTIR-microspectroscopy of stratum corneum single cells and stratum corneum tissue. *PCCP* 2002;4(22):5671–7.
- Bartick E, Schwartz R, Bhargava R, Schaeberle M, Fernandez D, Levin I. Spectral imaging of latent fingerprints. The Federation of Analytical Chemistry and Spectroscopy Societies, 29th Annual FACSS Meeting; October 13–17, 2002. Providence, RI. Santa Fe, NM: The Federation of Analytical and Spectroscopy Societies, 2002.
- Tahtouh M, Kalman JR, Roux C, Lennard CI, Reedy BJ. The detection and enhancement of latent fingerprints using infrared chemical imaging. *J Forensic Sci* 2005;50(1):64–72.
- Huffman SW, Brown CW. Multivariate analysis of infrared spectroscopic image data. In: Bhargava R, Levin I, editors. Spectrochemical analysis using infrared multichannel detectors. Ames: Blackwell Publishing Ltd., 2005:85–114.
- Marcott C, Reeder RC, Sweat JA, Panzer DD, Wetzel FT-IR spectroscopic imaging microscopy of wheat kernels using a Mercury–Cadmium–Telluride focal-plane array detector. *Vibrat Spectrosc* 1999;19:123–9.

Additional information and reprint requests:
Edward Bartick, Ph.D.
Department of Chemistry and Biochemistry
Suffolk University
41 Temple Street
Boston, MA 02114
E-mail: ebartick@suffolk.edu